

Proton Acceleration by High-Intensity UV Laser Irradiation with Thin Foil Targets

Eiichi Takahashi, Susumu Kato, Yuji Matsumoto,
and Isao Okuda

*National Institute of Advanced Industrial Science and Technology (AIST), 1-1-1 Umezono, Tsukuba Ibaraki 305-8568
Japan*

(Received: 1 September 2008 / Accepted: 26 December 2008)

Proton acceleration experiments by irradiation of intense ultra-violet lasers with thin foil targets were conducted. Energies and efficiencies of the accelerated protons were investigated over the target thickness from several μm to 50 nm using various materials. In order to irradiate the very thin foil targets, the discharge pre-amplifier in the previous system was removed to reduce amplified spontaneous emission which disturbed the main pulse interactions. A Thomson parabola ion spectrometer with CR39 plastic nuclear track detectors were used to observe spectra of the accelerated protons. The maximum energies and efficiencies of accelerated protons increased with decreasing the target thickness rather than the product of the density and thickness of the targets. These results were explained by a geometrical effect on hot electron recycling.

Keywords: Proton acceleration, KrF laser, UV, ultrahigh-intensity laser, TNSA, Coulomb explosion.

1. Introduction

Using short-pulse, ultrahigh-intensity lasers for generating fast-proton beams by irradiating thin foils is a new area of research, and has opened up applications such as proton radiography [1], radioisotope generators [2,3], and inertial confinement fusion [4]. An intense laser beam focused onto a thin foil target creates hot electrons that propagate through the target and induce a space-charge field when they exit. Because of this strong static-electric field, protons can be accelerated perpendicular to the target surface, which is the so-called target normal sheath acceleration mechanism (TNSA) [5].

Until now, the almost all proton acceleration experiments have only been conducted using infrared lasers, such as Nd:glass lasers at a wavelength of 1.06 μm [6] and Ti:sapphire lasers at a wavelength of 800 nm [7,8].

From a practical perspective, the use of short-wavelength lasers has advantages such as high contrast in the laser pulse and a better absorption rate for the intensity around 10^{18} W/cm^2 .

First, the contrast is very important for the intense laser-plasma interaction research. If we use an infrared laser oscillator for generation of seed pulses, nonlinear frequency conversion to short-wavelength provides the improvement of the contrast easily.

Second, assuming the compact laser system ($\sim 1 \text{ J}$, $\sim 100 \text{ fs}$), we estimated the peak focal intensity remains around the 10^{18} W/cm^2 . The short-wavelength laser interaction usually has a large rate of laser absorption for the intensity region. For example, according to the vacuum

heating model in reference [9], the rate of laser absorption increases by the formation of an under-dense plasma shelf, where the formation time is $t_{45^\circ}(\text{fs}) = 130(A/Z)^{1/2}\lambda_\mu$, and A , Z , and λ_μ , are the atomic mass, charge, and wavelength in μm , respectively. It takes only several tens of femto-seconds for ultraviolet lasers to form the self while more than a hundred femto-second for infrared lasers. In addition, the high-density generation of hot electrons is also expected using parametric scattering with an appropriate scale length of interacting plasmas, when using short-wavelength lasers [10].

In our previous paper, we reported the first proton acceleration experiment using an intense ultraviolet (UV) laser [11]. The highest proton energy of 700 keV was observed when the p-polarized laser irradiated the target of 4 μm copper foils. The maximum irradiation intensity on the target was $1.3 \times 10^{18} \text{ W/cm}^2$.

However, the proton acceleration efficiency was quite low, $\sim 10^{-4} \%$. This small efficiency was explained by the inefficient transmission of hot electrons through the copper target of 4 μm in thickness.

To increase the hot electron transmission, we tried to reduce the thickness of the target. Then, we found that the amplified spontaneous emission (ASE) from the discharge pre-amplifier in our previous system affected the results because the target would be destroyed before the interaction of the peak of laser pulse.

So, in this paper we report the proton acceleration using thinner target without using the discharge pumped

pre-amplifier to eliminate the ASE.

In section 2, we explain the experimental setup briefly. The key finding of this paper is the proton accelerations mainly dependent on the target thickness rather than the product of the density and thickness, which is illustrated in section 3. In section 4, one-dimensional particle-in-cell code with boosted frame method simulates the laser-plasma interactions of the current experimental conditions. These results are discussed in section 5.

2. Experimental Setup

The experimental setup is shown in Fig. 1. The seed laser pulses were generated using a Ti:sapphire laser operated at a wavelength of 745 nm. The pulses were frequency tripled using nonlinear optical crystals (THG), and amplified through an electron beam (E-beam)-pumped KrF laser amplifier. The E-beam amplifier has the aperture of 20 cm in diameter. The discharge KrF laser pre-amplifier had been located in between the THG and E-beam amplifier in previous paper but removed for current experiment.

The amplified 248-nm-wavelength KrF laser pulses had 400 fs in pulse duration and 250 mJ in energy. The peak intensity and the focal spot diameter were 5×10^{17} W/cm² and 14 μ m, respectively. The contrast of the amplified laser pulses was better than 10^9 . The intensity of the ASE from the e-beam amplifier was weak ($\sim 10^8$ W/cm² on target) because of its large illumination area.

The intensity reduction was almost factor of 3 and the contrast improvement was more than 1 order of magnitude by the removing of the discharge pre-amplifier.

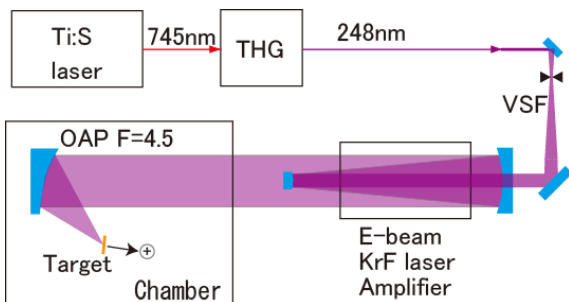


Fig.1 Illustration of the experimental setup. The

Ti:sapphire laser produced the seed laser pulses at a wavelength of 745 nm. The frequency-tripled pulses were amplified using electron-beam-pumped KrF laser amplifier.

CR39 plastic nuclear track detectors were used to record the accelerated protons. The CR39 was etched in a 6.25 N NaOH solution for 16 hours, maintaining the temperature at 70 °C to observe recorded proton traces. A Thomson parabola ion spectrometer was used to observe energy spectra of accelerated ions. The Thomson parabola

spectrometer was located at target normal of the rear side. The pinhole diameter of the spectrometer entrance was 100 μ m.

3. Results

The dependence of maximum proton energy on target thickness was shown in Fig. 2. The laser was directed onto the target at an incident angle of 30° with p-polarized light. The data point in the previous paper was also shown in the figure as a closed circle. Note that the peak intensity and contrast were different.

The maximum proton energy was inverse proportional to the thickness of the target rather than the product of density and thickness over the various target material we used. And increase of the energy with decreasing the thickness was almost saturated below the thickness of 1 μ m. The accelerated protons were still observed for the silicon-nitride membrane targets which had the thickness of 50 nm and 100 nm. In contrast to the experiment using previous setup; no proton had been observed for the 1 μ m copper targets.

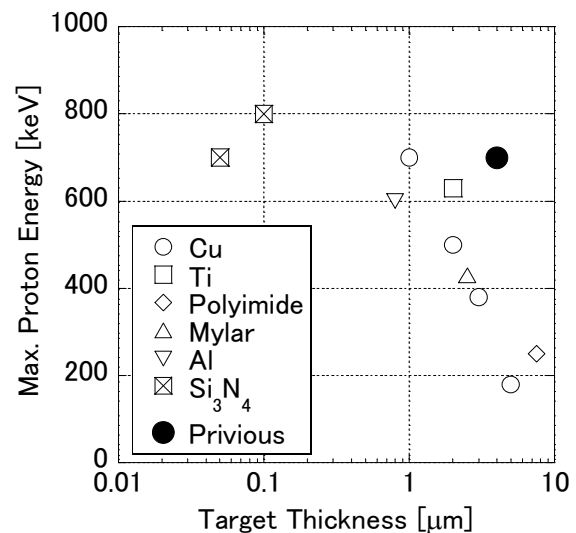


Fig.2 Maximum proton energy as a function of the target thickness at an irradiation intensity of 5×10^{17} W/cm². Previous result is also shown as closed circle. The intensity and contrast of the laser were different between the current and previous results.

The dependence of proton acceleration efficiency on the target thickness was also shown in Fig. 3. These efficiencies were estimated by assuming the uniform proton emission which had a divergence angle of 30°. This angle was estimated from the measurements of proton emission profile in previous experiments. The efficiencies were calculated by integrating the proton spectra from 200 keV to the maximum energy. Because most of the lower energy part of proton spectrum were saturated by the

overlapping of proton etch pits, these parts of the spectrum were extrapolated from the high energy region of the spectrum.

The efficiencies were also inverse proportional to the target thickness and increased monotonically with decreasing it. Especially for the membrane target realized more than 3 orders of magnitude larger efficiencies compared to previous one.

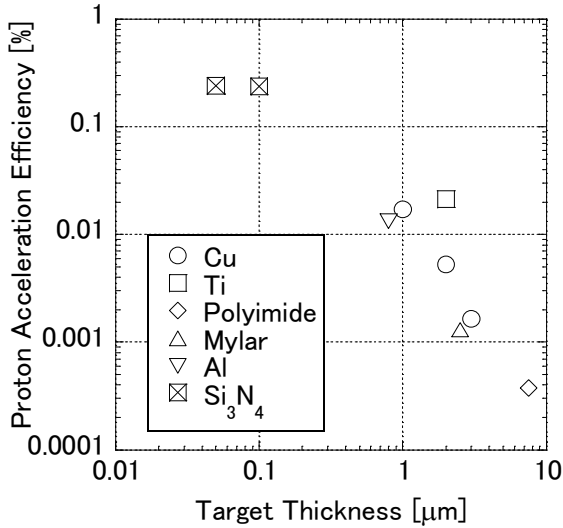


Fig.3 Proton acceleration efficiency as a function of the target thickness. The efficiency was estimated by assuming the proton emission angle of 30° .

4. Particle-in-cell code simulation

Interaction of the UV laser pulse with thin foil targets at an incident angle of 30° was investigated using a one dimensional particle-in-cell (1D PIC) simulation code. The results of the simulation for normal incidence had been reported in Reference [10].

The parameters of the simulation are almost same as before except for the incident angle of laser. The laser pulses have a waveform of a sine-squared envelope with duration of 800 fs (i.e. the width at half maximum is 400 fs). Preformed plasma sets are positioned at the front of the laser incidence. The preformed plasma, where $A = 12$ and $Z = 6$, has temperature 1 keV and an exponentially decreasing density profile $n_0 \exp(-x/L)$, where $n_0 = 2 \times 10^{22} \text{ cm}^{-3}$ is the electron density at the interface between the thin target and preformed plasma, and L was the scale length of the preformed plasma. The scale length is varied from $L = 0.001$ – 2 m . Protons are positioned behind the rear surface to investigate ion acceleration because of a high-energy electron sheath formed at the rear surface.

The protons have a density and thickness of $1 \times 10^{22} \text{ cm}^{-3}$ and 0.1 m , respectively. At all scale length, the laser pulse interacts with the preformed plasmas at a critical density, this implies, the pulse does not interact with the

solid target. Electron transport in a solid density target is assumed not to be affected by the target material.

Fig. 4 shows the snap shot of maximum proton energies at the time of 400 fs as a function of the scale length of the interacting plasma which is one of the most uncertain parameters. The peaks of the energy were observed at the scale length of 0.25 μm for all irradiation intensities, which suggest the resonance absorption. Even for shorter scale lengths below 0.01 μm , protons were still accelerated. This behavior can be explained by the formation of an under-dense plasma shelf for long pulse interactions [9].

We set the snap shot time of the simulation at 400 fs by watching the acceleration length in the simulation. Because the focal spot diameter was 10 μm , one-dimensional acceleration can be expected until the acceleration length of around 1 μm . High energy protons could be observed by increasing the acceleration duration.

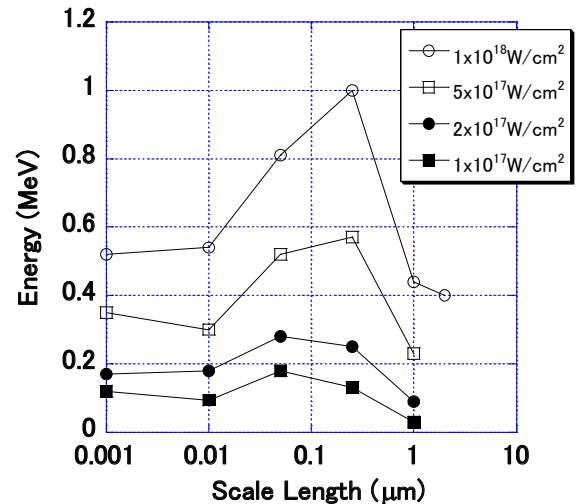


Fig.4 Dependence of maximum proton energies on scale lengths of the plasmas by PIC code simulations ($t = 400$ fs). The incident angle of the laser was assumed to be 30° from the target normal.

5. Discussion

The maximum proton energy obtained by the experiment was almost reproduced by the PIC simulation for the intensity of $5 \times 10^{17} \text{ W/cm}^2$ for the scale length around 0.1 μm . This proton energy is also comparable to the energy of protons accelerated by high-intensity 0.53 μm lasers reported in reference [2].

The key finding of this paper is the proton accelerations mainly dependent on the target thickness rather than the product of the density and thickness. This implies that a geometrical effect should be important for the behavior rather than classical or anomalous attenuation of hot electrons in the target material for our current

experiments. Because the variation of the target density is very large (Cu: 8.92 g/cm³, Al: 2.7 g/cm³, Mylar: 1.3g/cm³), classical attenuation should be negligibly small. Provided that hot electron energies above 200 keV, the hot electron can transmit without losing energy for most of the target material and thickness we used.

The geometrical effect on the hot electron recycling can explain the behavior. The hot electrons created at the front side of the target propagated through the target; the electrons were expected to return from the sheath potential at the rear side to the region of laser-plasma interactions. If these electrons propagate obliquely, they would not return under the certain conditions. So, taking account of the focal spot diameter of 10 μm and the oblique generation of hot electron, the target thickness should be 1 μm or less to realize efficient electron recycling. It is also reasonable for the model that the proton energies are saturated below 1 μm . The maximum energy of the protons for the 50 nm thick Si₃N₄ target was lower than the 100 nm thick Si₃N₄ target. The most plausible explanation for the behavior is the insufficient laser contrast to irradiate such an ultra-thin target.

The simulation of PIC code supported the oblique generation; the direction of the hot electrons was closer to the laser axis even for the resonance absorption conditions. This result suggests that not only the electrostatic field but also electromagnetic field contributed the electron acceleration.

The efficiency increased monotonically as the thickness decreased. Even for the membrane targets, our maximum efficiency of 0.25 % was lower than the efficiency of 4 % reported by the other acceleration experiment using membrane targets [12]. There is a possibility that the physics of our proton acceleration for the membrane targets was closer to Coulomb explosion [13] rather than the TNSA due to the long irradiation time. Further experiment is necessary to investigate it by observing the proton emission profiles.

Additionally, because of the observation of proton emission by the use of membrane targets, the frequency tripling was also shown as effective contrast improving method.

6. Summary

Proton acceleration experiments by irradiation of intense ultra-violet lasers with thin foil targets were conducted. Energies and efficiencies of the accelerated protons were investigated over the target thickness from several μm to 50 nm using various materials. It was found that the maximum energies and efficiencies of accelerated protons increased as the target thickness decreased rather than the product of the density and thickness of the targets. The behavior was explained by the geometrical inefficient recycling of hot electrons.

Acknowledgement

This study was financially supported by the Budget for Nuclear Research of the Ministry of Education, Culture, Sports, Science and Technology, based on the screening and counseling by the Atomic Energy Commission.

7. References

- [1] A. J. Mackinnon, et al., Phys. Rev. Lett. 97, 045001 (2006).
- [2] K. Nemoto, et al., Appl. Phys. Lett. 78, 595 (2001).
- [3] S. Fritzler, et al., Appl. Phys. Lett. 83, 3039 (2003).
- [4] M. Roth, et al., Phys. Rev. Lett. 86, 436 (2001).
- [5] S. C. Wilks, et al., Phys. Plasmas 8, 542 (2001).
- [6] R. A. Snavely, et al., Phys. Rev. Lett. 85, 2945 (2000).
- [7] A. J. Mackinnon, et al., Phys. Rev. Lett. 88, 215006 (2002).
- [8] T. Nayuki, et al., J. Appl. Phys. 100, 043111 (2006).
- [9] P. Gibbon, Phys. Rev. Lett. 73, 664 (1994).
- [10] S. Kato, et al., Plasma Fusion Res. 2, 032 (2007).
- [11] E. Takahashi, et. al., Plasma Fusion Res. 3, 024 (2008).
- [12] P. Antici, et. al., Phys. Plasmas 14, 30701 (2007).
- [13] S. Okihara, et. al., J. Nucl. Sci. Tech. 39, 1 (2002).